
SIMBA: A SCALABLE BILEVEL PRECONDITIONED GRADIENT METHOD FOR FAST EVASION OF FLAT AREAS AND SADDLE POINTS

A PREPRINT

Nick Tsipinakis

Department of Mathematics
UniDistance Suisse
Brig, Switzerland

nikolaos.tsipinakis@unidistance.ch

Panos Parpas

Department of Computing
Imperial College London
London, UK

panos.parpas@imperial.ac.uk

September 12, 2023

ABSTRACT

The convergence behaviour of first-order methods can be severely slowed down when applied to high-dimensional non-convex functions due to the presence of saddle points. If, additionally, the saddles are surrounded by large plateaus, it is highly likely that the first-order methods will converge to sub-optimal solutions. In machine learning applications, sub-optimal solutions mean poor generalization performance. They are also related to the issue of hyper-parameter tuning, since, in the pursuit of solutions that yield lower errors, a tremendous amount of time is required on selecting the hyper-parameters appropriately. A natural way to tackle the limitations of first-order methods is to employ the Hessian information. However, methods that incorporate the Hessian do not scale or, if they do, they are very slow for modern applications. Here, we propose Simba, a scalable preconditioned gradient method, to address the main limitations of the first-order methods. The method is very simple to implement. It maintains a single precondition matrix that it is constructed as the outer product of the moving average of the gradients. To significantly reduce the computational cost of forming and inverting the preconditioner, we draw links with the multilevel optimization methods. These links enables us to construct preconditioners in a randomized manner. Our numerical experiments verify the scalability of Simba as well as its efficacy near saddles and flat areas. Further, we demonstrate that Simba offers a satisfactory generalization performance on standard benchmark residual networks. We also analyze Simba and show its linear convergence rate for strongly convex functions.

Keywords saddle free optimization · preconditioned gradient methods · coarse-grained models · deep learning

1 Introduction

We focus on solving the following optimization problem, commonly referred to as empirical risk minimization:

$$\min_{\mathbf{x} \in \mathbb{R}^n} f(\mathbf{x}) := \frac{1}{m} \sum_{i=1}^m f_i(\mathbf{x}). \quad (1)$$

We assume that the model parameters are available in a *decoupled* form, that is, $\mathbf{x} = \{\mathbf{x}^l : l = 1, \dots, L\}$, for some positive integer L . The decoupled parameter setting naturally emerges for the training of a deep neural network (DNN) where L corresponds to the number of layers. In large-scale optimization scenarios, stochastic gradient descent method (SGD) and its variants have become a standard tool due to their simplicity and low per-iteration and memory costs. While easy to implement, they are nevertheless accompanied with important shortcomings. Below, we discuss these limitations and argue that they mainly stem from the absence of the Hessian matrix (or an appropriate approximation that leverages its structural properties) in their iterative scheme.

Shortfall I: Slow evasion of saddle points. The prevalence of saddle points in high dimensional neural networks has been examined in the past and it has been shown that the number of saddles increases exponentially with the dimension n Dauphin et al. [2014]. Consequently, developing algorithms that are capable of escaping saddle points is a primary goal when it comes to the training of DNNs. While stochastic first-order methods have theoretical guarantees of escaping saddle points almost always Panageas et al. [2019], it remains unclear whether they can achieve this efficiently in practice. As a result, given the significantly larger number of saddle points compared to local minima in high-dimensional settings, it is likely that stochastic first-order methods will converge to a saddle point rather than the desired local minimum. The most natural way to ensure convergence to a local minimum in the presence of saddles is by incorporating the Hessian matrix to scale the gradient vector. The Cubic Newton Nesterov et al. [2018] is a key method in non-convex optimization known to be able to escape saddles in a single iteration resulting in rapid convergence to a local minimum. The Cubic Newton method achieves this using the inverse of a regularized version of the Hessian matrix to premultiply the gradient vector. However, the method has expensive iterates and does not scale in high dimensions. Nevertheless, its theory indicates that methods employing accurate approximations of the regularized Hessian are expected to effectively evade saddle points and converge rapidly.

Shortfall II: Slow convergence rate near flat areas and the vanishing gradient issue. The convergence behaviour of first-order methods can be significantly affected near local minima that are surrounded by plateaus Boyd and Vandenberghe [2004], Nesterov [2004]. For instance, this occurs, when its Hessian matrix has most of the eigenvalues equal to zero. Therefore, to effectively navigate on such a flat landscape is to employ the inverse Hessian matrix. For instance, the Newton method pre-multiplies the gradient with the inverse Hessian to perform a local change of coordinates which significantly accelerates the convergence rate. Intuitively, one can expect a similar convergence behaviour by replacing the Hessian matrix with a preconditioned matrix that retains its structure. On the other hand, the vanishing gradient issue is commonly observed in the training of DNNs for which activation functions that range in $[0, 1]$ are required. In such cases, the gradient value computed through the back-propagation decreases exponentially as the number of layers L of the network increase yielding no progress for the SGD. Hence, similar to addressing the slow-convergence issue near flat areas, employing a preconditioner is expected to mitigate the vanishing gradient issue and thus accelerate the convergence of the SGD method.

To tackle the above shortfalls, the diagonal (first- or second-order) methods were introduced Duchi et al. [2011], Tieleman et al. [2012], Zeiler [2012], Kingma and Ba [2014], Zaheer et al. [2018], Yao et al. [2021], Ma [2020], Jahani et al. [2021], Liu et al. [2023]. These algorithms aim to improve the behavior of the SGD near saddles or flat areas by preconditioning the gradient with a diagonal vector that mimics the hessian matrix. However, the Hessian matrices of deep neural networks need not be sparse, which means that a diagonal approximation of the Hessian may be inadequate. This raises concerns about the ability of diagonal methods to converge to a local minimum. A more promising class of algorithms consists of those preconditioned gradient methods that maintain a matrix instead of the potentially poor diagonal approximation. As noted earlier, the Cubic Newton method can effectively address the aforementioned shortfalls but it does not scale in large-scale settings. Other methods that explicitly use or exploit the Hessian matrix, such as Newton or Quasi-Newton methods Nesterov [2004], Broyden [1967], or those based on randomization and sketching Erdogdu and Montanari [2015], Pilanci and Wainwright [2017], Xu et al. [2016, 2020] still suffer from the same limitations as the Cubic Newton. A potentially promising way to address the storage and computational limitations of the Newton type methods is to employ precondition matrices based on the first-order information Duchi et al. [2011], Gupta et al. [2018]. However, to the best of our knowledge, the performance of such methods near saddles or flat areas is yet to be examined. Another possible solution is to utilize the multilevel framework in optimization which significantly reduces the cost of forming and inverting the Hessian matrix Tsipinakis and Parpas [2021], Tsipinakis et al. [2023]. But, it remains unclear whether the multilevel Newton-type methods can be efficiently applied to the training of modern deep neural networks.

In this work, we introduce Simba, a **Scalable Iterative Minimization Bilevel Algorithm** that addresses the above shortfalls and scales to high dimensions. The method is very simple to implement. It maintains a precondition matrix where its inverse square root is used to premultiply the moving average of the gradient. In particular, the precondition matrix is defined as the outer product of the exponential moving average (EMA) of the gradients. We explore the link between the multilevel optimization methods and the preconditioned gradient methods which enables us to construct preconditioners in a randomized manner. By leveraging this connection, we significantly reduce the cost and memory requirements of these methods to make them more efficient in time for large-scale settings. We propose performing a Truncated Singular Value decomposition (T-SVD) before constructing the inverse square root preconditioner. Here, we retain only the first few, say r , eigenvalues and set the remaining eigenvalues equal to the r^{th} eigenvalue. This approach aims to construct meaningful preconditioners that do not allow for zero eigenvalues, and thus expecting a faster escape rate from saddles or flat areas. Our algorithm is inspired by SigmaSVD Tsipinakis et al. [2023], Shampoo Gupta et al. [2018] and SGD with momentum Bubeck et al. [2015]. Simba is presented in Algorithm 1. A Pytorch implementation of Simba is available at <https://github.com/Ntsip/simba>.

Algorithm 1 Simba. Proposed default hyper-parameters: \mathbf{R}_k as in Definition 2.1, $t_k = 10^{-2}$, $b = 0.9$, $r = 20$, $n_\ell = 0.5n$, $m = 10^{-8}$.

Require: t_k (step-size), $\beta \in (0, 1)$ (momentum), \mathbf{x}_0 - (initial point), r (No of eigenvalues), n_ℓ (coarse model dimensions), m (eigenvalue correction).

Set $\mathbf{G}_0 = 0$

for $k = 1, 2, \dots$ **do**

$\mathbf{G}_k = \beta \mathbf{G}_{k-1} + \nabla f(\mathbf{x}_{k-1})$ (EMA of gradients)

$\mathbf{G}_{\ell,k} = \mathbf{R}_k \mathbf{G}_k$ (coarse EMA of gradients)

$\mathbf{Q}_{\ell,k} = \mathbf{G}_{\ell,k} \mathbf{G}_{\ell,k}^T$ (EMA-based preconditioner)

$[\mathbf{U}_{r+1} \mathbf{\Lambda}_{r+1}] = \text{T-SVD}(\mathbf{Q}_{\ell,k})$ by Halko et al. [2011]

$[\mathbf{\Lambda}_{r+1}]_{i,m} = \begin{cases} \mathbf{\Lambda}_i, & \mathbf{\Lambda}_i \geq m \\ m, & \text{otherwise} \end{cases}, \quad \text{and form } \mathbf{\Lambda}_{r+1}^m$

$\mathbf{Q}_{\ell,k}^{-\frac{1}{2}} = [\mathbf{\Lambda}_{r+1}]_{r+1,m}^{-\frac{1}{2}} \mathbf{I}_{n_\ell} + \mathbf{U}_r \left([\mathbf{\Lambda}_{r+1}^m]^{-\frac{1}{2}} - [\mathbf{\Lambda}_{r+1}]_{r+1,m}^{-\frac{1}{2}} \mathbf{I}_r \right) \mathbf{U}_r^T$

$\mathbf{x}_{k+1} = \mathbf{x}_k - t_k \mathbf{P}_k \mathbf{Q}_{\ell,k}^{-\frac{1}{2}} \mathbf{R}_k \mathbf{G}_k$

end for

1.1 Related Work

The works most closely related to ours is Shampoo Gupta et al. [2018] and AdaGrad Duchi et al. [2011]. However, both methods have important differences to our approach which are discussed below. AdaGrad is an innovative adaptive first-order method which performs elementwise division of the gradient with the square root of the accumulated squared gradient. Adagrad is known to be suitable for sparse settings. However, the version of the method that retains a full preconditioner matrix is rarely used in practice due to the increased computational cost. Moreover, Shampoo, unlike our approach, maintains multiple preconditioners, one for each tensor dimension (i.e., two for matrices while we always use one). In addition, it computes a full SVD for each preconditioner. Further, all preconditioners lie in the original space dimensions. Given the previous considerations, Shampoo becomes computationally expensive when applied to very large DNNs. In contrast, our algorithm addresses the computational issues of Shampoo. Another difference between Shampoo and our approach is the way the preconditioners are defined. Shampoo defines the preconditioners as a sum of the outer product of gradients, whereas we employ the exponential moving average. In addition, the performance of Shampoo around saddles and flat areas is yet to be examined. We conjecture that Shampoo may not effectively improve the behaviour of the first-order methods near plateaus due to the monotonic increase of the eigenvalues in the preconditioners.

Hessian-based preconditioned methods have been also proposed to improve convergence of the optimization methods near saddle point Reddi et al. [2018], Dauphin et al. [2014], O’Leary-Roseberry et al. [2020]. However, these methods rely on second-order information which can be prohibitively expensive for very large DNNs. Therefore, they are more suitable to apply in conjunction with a fast first-order method and employ the Hessian approximation when first-order methods slow down. However, our method is efficient from the beginning of the training. A notable second-order optimization method is K-FAC Martens and Grosse [2015]. K-FAC approximates the Fisher information matrix of each layer using the Kronecker product of two smaller matrices that are easier to handle. However, K-FAC is specifically designed for the training of generative (deep) models while our method is general and applicable to any stochastic optimization regime.

As far as the adaptive diagonal methods are concerned, Adam and RMSprop were introduced to alleviate the limitations of AdaGrad. RMSprop scales the gradient using an averaging of the squared gradient. On the other hand, Adam scales the EMA of the gradient by the EMA of the squared gradient. Adam iterations has been shown to significantly improve the performance of first-order diagonal methods in the optimization of DNNs. Another method, named Yogi, has similar updates as AdaGrad but allows for the accumulated squared root not be monotonically increasing. To provide EMA of the gradient with a more informative scaling, several approaches have been proposed that replace the squared gradient with an approximation of the diagonal of the Hessian matrix Jahani et al. [2021], Yao et al. [2021], Ma [2020]. AdaHessian Yao et al. [2021] approximates the Hessian matrix by its diagonal matrix using the Hutchinson’s method while Apollo Ma [2020] based on the variational technique using the weak secant equation. Further, OASIS Jahani et al. [2021] is an adaptive modification of AdaHessian that automatically adjusts learning rates. A recent work called Sophia Liu et al. [2023] modifies AdaHessian direction by clipping it by a scalar. The authors also provide alternatives on the diagonal Hessian matrix approximation which they suggest to compute every 10 iterations to reduce the computational

costs. However, it is still unclear whether the diagonal methods offer satisfactory performance near saddles points and flat areas, or if they effectively tackle the vanishing gradient issue in practical applications.

1.2 Contributions

The main contribution of this paper is the development of a scalable method that addresses the aforementioned shortfalls by empirical evidence. The method is scalable for training DNNs as it maintains only one preconditioned matrix at each iteration which lies in the subspace (coarse level). Thus, we significantly reduce the cost of forming and computing the SVD compared to Shampoo. The fact that we use a randomized T-SVD and requiring the most informative eigenvalues further reduces the total computational cost. The numerical experiments demonstrate that Simba can have cheaper iterates than AdaHessian and Shampoo in large-scale settings and deep architectures. In particular, in these scenarios, the wall-clock time of our method can be as much as 25 times less than Shampoo and 2 times less than AdaHessian. We, in addition, illustrate that Simba offers comparable, if not better, generalization errors against the state-of-the-art methods in standard benchmark ResNet architectures.

Further, the numerical experiments show that our method has between two and three times more expensive iterates than Adam. This is expected due to outer products and the randomized T-SVD. However, this is a reasonable price to pay to improve the escape rate from saddles and flat areas of the existing preconditioned gradient methods. Therefore, Simba is suitable in problems where diagonal methods suffer from at least one of the previous shortfalls. In such cases, we demonstrate that diagonal methods require much larger wall-clock time to reach an error as low as our method achieves. Hence, we argue that, besides the encouraging preliminary empirical results achieved by Simba, this paper highlights the limitations of diagonal methods, which are likely to get trapped near saddle points and thus return sub-optimal solution, particularly in the presence of large plateaus. This emphasizes the need to develop scalable algorithms that utilize more sophisticated preconditioners instead of relying on poor diagonal approximations of the Hessian matrix. Simba is accompanied with a simple convergence analysis assuming strongly convex functions.

2 Description of the Algorithm

In this section, we begin by discussing the standard Newton-type multilevel method and its main components, i.e., the hierarchy of coarse models and the linear operators that will be used to transfer information from coarse to fine model and vice versa. Then, as all the necessary ingredients are in place, we present the proposed algorithm. Even though, we assume a bilevel hierarchy, extending Simba to several level is straightforward.

2.1 Background Knowledge - Multilevel Methods

We will be using the multilevel terminology to denote f as the *fine* model and also assume that a *coarse* model that lies in lower dimensions is available. In particular, the coarse model is a mapping $F : \mathbb{R}^{n_\ell} \rightarrow \mathbb{R}$, where $n_\ell < n$. The subscript ℓ will be used to denote quantities, i.e., vectors and scalars, that belong to the coarse level. We assume that both fine and coarse models are bounded from below so that a minimizer exists.

In order to reduce the computational complexity of Newton type methods, the standard multilevel method attempts to solve (1) by minimizing the coarse model to obtain search directions. This process is described as follows. First, one needs to have access to linear prolongation and restriction operators to transfer information from the fine to coarse model and vice versa. We denote $\mathbf{P} \in \mathbb{R}^{n \times n_\ell}$ be the prolongation and $\mathbf{R} \in \mathbb{R}^{n_\ell \times n}$ the restriction operator and assume that they are full rank and $\mathbf{P} = \mathbf{R}^T$. Given a point \mathbf{x}_k at iteration k , we move to the coarse level with initialization point $\mathbf{y}_0 = \mathbf{R}\mathbf{x}_k$. Subsequently, we minimize the coarse model F to obtain \mathbf{y}^* and construct a search direction by:

$$\mathbf{d}_k := \mathbf{P}_k(\mathbf{y}^* - \mathbf{y}_0). \quad (2)$$

To compute the search directions effectively, the standard multilevel method considers the Galerkin model as a choice of the coarse model:

$$F(\mathbf{y}) := \langle \mathbf{R}_k \nabla f(\mathbf{x}_k), \mathbf{y} - \mathbf{y}_0 \rangle + \frac{1}{2} \langle \mathbf{R}_k \nabla^2 f(\mathbf{x}_k) \mathbf{P}_k (\mathbf{y} - \mathbf{y}_0), \mathbf{y} - \mathbf{y}_0 \rangle. \quad (3)$$

It can be shown that combining (2) and (3) we obtain a closed form solution for the coarse direction:

$$\mathbf{d}_k = -\mathbf{P}_k (\mathbf{R}_k \nabla^2 f(\mathbf{x}_k) \mathbf{P}_k)^{-1} \mathbf{R}_k \nabla f(\mathbf{x}_k)$$

However, it may be ineffective to employ solely the above strategy when computing the search direction if \mathbf{R} is fixed or defined in a deterministic fashion at each iteration. For instance, this can occur when $\nabla f(\mathbf{x}) \in \text{null}(\mathbf{R})$ while

$\|\nabla f(\mathbf{x}_k)\|_2 \neq 0$, which implies no progress for the multilevel algorithm. The following conditions were introduced to prevent the multilevel algorithm from taking an ineffective coarse step:

$$\|\mathbf{R}\nabla f(\mathbf{x})\| > \xi\|\nabla f(\mathbf{x})\| \quad \text{and} \quad \|\mathbf{R}\nabla f(\mathbf{x})\| > e,$$

where $\xi \in (0, \min(1, \|\mathbf{R}\|))$ and $e > 0$ are user defined parameters. Thus, the standard multilevel algorithm computes the coarse direction when the above conditions are satisfied and the fine direction (Newton) otherwise. On the other hand, it is expected that the multilevel algorithm will construct effective coarse directions when \mathbf{R} is selected randomly at each iteration. In particular, it has been demonstrated that the standard multilevel method can perform always coarse steps without compromising its superlinear or composite convergence rate (see for example Ho et al. [2019], Tsipinakis and Parpas [2021], Tsipinakis et al. [2023]).

2.2 Simba

The standard multilevel algorithm is well suited for strictly convex functions since the Hessian matrix is always positive definite. Due to the absence of positive-definiteness in general non-convex problems, Newton type methods may converge to a saddle point or a local maximum since they cannot guarantee the descent property of the search directions. They can even break down when the Hessian matrix is singular. These limitations have been efficiently tackled in the recent studies Nesterov and Polyak [2006]. In multilevel literature, SigmaSVD Tsipinakis et al. [2023] addresses these limitations by using a truncated low-rank modification of the standard multilevel algorithm that efficiently escapes saddle points and flat areas. While SigmaSVD has been shown to perform well near saddles and flat areas, it requires $\mathcal{O}(mn_\ell^2)$ operations to form the reduced Hessian matrix which is prohibitively expensive for modern deep neural network models. Here, to alleviate this burden, we replace the expensive Hessian matrix with the outer product of the gradients. For this purpose, we consider the following coarse model:

$$F(\mathbf{y}) := \langle \mathbf{R}_k \mathbf{G}_k, \mathbf{y} - \mathbf{y}_0 \rangle + \frac{1}{2} \langle (\mathbf{R}_k \mathbf{H}_k \mathbf{P}_k)^{\frac{1}{2}} (\mathbf{y} - \mathbf{y}_0), \mathbf{y} - \mathbf{y}_0 \rangle, \quad (4)$$

where $\mathbf{H}_k := \mathbf{G}_k \mathbf{G}_k^T$ and $\mathbf{G}_k := \nabla f(\mathbf{x}_k)$. Thus, by defining $\hat{\mathbf{d}}_\ell := \mathbf{y}^* - \mathbf{y}_0$ and $\mathbf{Q}_{\ell,k} := \mathbf{R}_k \mathbf{H}_k \mathbf{P}_k$, the coarse direction can be computed explicitly:

$$\begin{aligned} \hat{\mathbf{d}}_k &= \mathbf{P}_k \left(\arg \min_{\mathbf{d}_\ell \in \mathbb{R}^{n_\ell}} \langle \mathbf{R}_k \mathbf{G}_k, \mathbf{d}_\ell \rangle + \frac{1}{2} \langle \mathbf{Q}_{\ell,k}^{\frac{1}{2}} \mathbf{d}_\ell, \mathbf{d}_\ell \rangle \right) \\ &= -\mathbf{P}_k \mathbf{Q}_{\ell,k}^{-\frac{1}{2}} \mathbf{R}_k \mathbf{G}_k. \end{aligned}$$

To construct $\mathbf{Q}_{\ell,k}^{-\frac{1}{2}}$, we perform a randomized truncated SVD to obtain the first $r + 1$ eigenvalues and eigenvectors, that is, $[\mathbf{U}_{r+1}, \mathbf{\Lambda}_{r+1}] = \text{T-SVD}(\mathbf{Q}_{\ell,k})$ Halko et al. [2011]. Subsequently, we bound the diagonal matrix of eigenvalues from below by a scalar $m > 0$:

$$[\mathbf{\Lambda}_{r+1}]_{i,m} := \begin{cases} \Lambda_i, & \Lambda_i \geq m \\ m, & \text{otherwise,} \end{cases} \quad (5)$$

to obtain the new modified diagonal matrix as $\mathbf{\Lambda}_{r+1}^m$. We then construct $\mathbf{Q}_{\ell,k}^{-\frac{1}{2}}$ by treating all its eigenvalues below the r -th equal to $r + 1$ eigenvalue. Formally, we define

$$\mathbf{Q}_{\ell,k}^{-\frac{1}{2}} := [\mathbf{\Lambda}_{r+1}]_{r+1,m}^{-\frac{1}{2}} \mathbf{I}_{n_\ell} + \mathbf{U}_r \left([\mathbf{\Lambda}_{r+1}^m]^{-\frac{1}{2}} - [\mathbf{\Lambda}_{r+1}]_{r+1,m}^{-\frac{1}{2}} \right) \mathbf{U}_r^T. \quad (6)$$

The key component when forming the precondition matrix as above is that we do not allow for zero eigenvalues since zero eigenvalues indicate the presence of flat areas where the convergence rate of optimization methods significantly decays. Hence, by requiring $\mathbf{Q}_{\ell,k} \succeq m \mathbf{I}_{n_\ell}$, we ensure that directions which correspond to flat curvatures will turn into directions whose curvature is positive, anticipating an accelerated convergence to the local minimum or a fast escape rate from saddles. Similar techniques for constructing the preconditioners have been employed in Tsipinakis et al. [2023], Paternain et al. [2019] where it is demonstrated numerically that the algorithms can rapidly escape saddle points and flat areas in practical applications. The computational cost of forming the preconditioner matrix is $\mathcal{O}(n_\ell^2)$ which is significantly smaller than computing the Hessian matrix. Moreover, the randomized SVD requires $\mathcal{O}(rn_\ell^2)$ operation.

In addition, the method can be trivially modified to employ the EMA of the gradients to account for the averaged history of the local information. Moreover, the EMA of the gradient is used to construct more informative preconditioner matrices. Specifically, to obtain the accelerated algorithm, we set a momentum parameter $\beta \in (0, 1)$ and replace \mathbf{G}_k in (4) with the EMA update:

$$\mathbf{G}_k := \beta \mathbf{G}_{k-1} + \nabla f(\mathbf{x}_k),$$

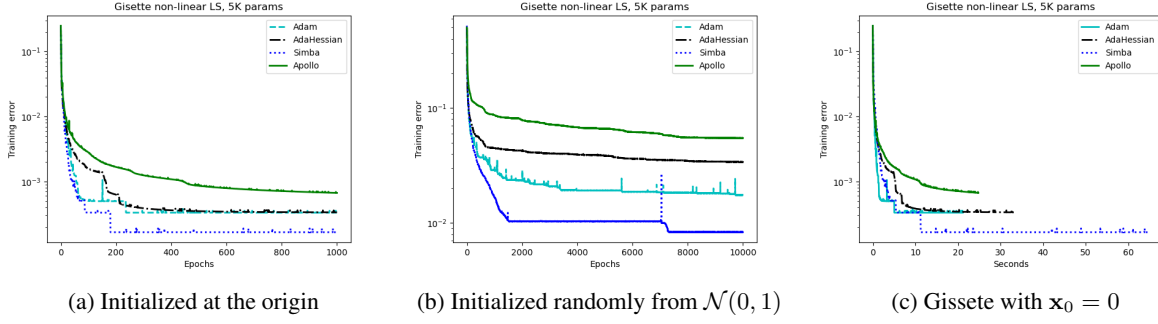


Figure 1: Convergence behaviour of various algorithms for the non-linear least-squares problem.

where $\mathbf{G}_0 = 0$ and $k \geq 1$. Simba with momentum is presented in Algorithm 1.

We emphasize that the method is scalable for solving large deep neural network models. We describe the three components that render the iterations of Simba efficient: **(a)** The operations can be performed in a decoupled manner. This means that preconditioners can be computed independently at each layer, leading into forming much smaller matrices that can be efficiently stored during the training. **(b)** The restriction operator is constructed based on uniform sampling without replacement from the rows of the identity matrix, \mathbf{I}_n . This is described formally in the following definition:

Definition 2.1. Let the set $S_n = \{1, 2, \dots, n\}$. Sample uniformly without replacement $n_\ell < n$ elements from S_n to construct $S_{n_\ell} = \{s_{n_1}, s_{n_2}, \dots, s_{n_\ell}\}$. Then, the i^{th} row of \mathbf{R} is the $s_{n_i}^{\text{th}}$ row of the identity matrix \mathbf{I}_n and $\mathbf{P} = \mathbf{R}^T$.

This way of constructing the restriction operator yields efficient iterations since in practice the coarse model in (4) can be formed by merely sampling n_ℓ elements from \mathbf{x}_k and $\nabla f(\mathbf{x}_k)$ which has negligible computational cost. **(c)** Taking advantage of the parameter structure. Methods that employ full matrix preconditioners further reduce the memory requirement by exploiting the matrix or tensor structure of the parameters (for details see Shampoo Gupta et al. [2018]). For instance, for a matrix setting, if the parameter $\mathbf{X} \in \mathbb{R}^{q \times d}$ and select $\mathbf{R} \in \mathbb{R}^{n_\ell \times q}$, where $n_\ell < q$, then we obtain $\mathbf{G}_{\ell,k} := \mathbf{R}\mathbf{G}_k \in \mathbb{R}^{n_\ell \times d}$ and $\mathbf{Q}_{\ell,k} \in \mathbb{R}^{n_\ell \times n_\ell}$. This results in $\mathcal{O}((r+d)n_\ell^2)$ operations for forming the preconditioner and applying the randomized SVD. Note that this number is much smaller than $\mathcal{O}((d+q)(d^2+q^2))$ of Shampoo.

3 Convergence Analysis

In this section we provide a simple convergence analysis of Simba when it generates sequences using the coarse model in (4) (without momentum). We show a linear convergence rate when the coarse model is constructed in both deterministic and randomized manner. Our analysis is based on the classical theory that assumes strongly convex functions and Lipschitz continuous gradients. In deterministic scenarios, the method is expected to alternate between coarse and fine steps to always reduce the value function. For this reason, we present two convergence results: **(a)** when the coarse step is always accepted, and **(b)** when only fine steps are taken. Hence the complete convergence behaviour of Simba is provided. On the other hand, when the prolongation operator is defined randomly at each iteration, multilevel methods expected to converge using coarse steps only Ho et al. [2019], Tsipinakis and Pappas [2021], Tsipinakis et al. [2023]. Our numerical experiments also verify this observation. Moreover, we derive the number of steps needed for the method to reach accuracy $\epsilon > 0$ for both cases. We begin by stating our assumptions.

Assumption 3.1. There are scalars $0 < \mu < L < +\infty$ such that f is μ -strongly convex and has L -Lipschitz continuous gradients if and only if:

1. (L -Lipschitz continuity) for all $\mathbf{x}, \mathbf{y} \in \mathbb{R}^n$

$$\|\nabla f(\mathbf{y}) - \nabla f(\mathbf{x})\|_2 \leq L\|\mathbf{y} - \mathbf{x}\|_2$$

2. (μ -strong convexity) for all $\mathbf{x}, \mathbf{y} \in \mathbb{R}^n$

$$f(\mathbf{y}) \geq f(\mathbf{x}) + \langle \nabla f(\mathbf{x}), \mathbf{y} - \mathbf{x} \rangle + \frac{\mu}{2}\|\mathbf{y} - \mathbf{x}\|_2^2$$

Next we state the assumptions on the prolongation and restriction operators.

Assumption 3.2. For the restriction and prolongation operators \mathbf{R} and \mathbf{P} it holds that $\mathbf{P} = \mathbf{R}^T$ and $\text{rank}(\mathbf{P}) = n_\ell$.

The assumptions on the linear operators are not restrictive for practical application. For instance, Definition 2.1 on \mathbf{P} and \mathbf{R} satisfies Assumption 3.2. The following assumption ensures that the algorithm always selects effective coarse directions.

Assumption 3.3. *There exist $e > 0$ and $\xi \in (0, \min(1, \|\mathbf{R}\|_2))$ such that if $\|\nabla f(\mathbf{x})\|_2 \neq 0$ it holds*

$$\|\mathbf{R}\nabla f(\mathbf{x})\|_2 > \xi\|\nabla f(\mathbf{x})\|_2 \quad \text{and} \quad \|\mathbf{R}\nabla f(\mathbf{x})\|_2 > e.$$

For our convergence result below we will need the following quantity: we denote $\omega := \max\{\|\mathbf{R}\|_2, \|\mathbf{P}\|_2\}$.

Theorem 3.4. *Let $f : \mathbb{R}^n \rightarrow \mathbb{R}$ be a function such that Assumption 3.1 holds. Suppose also that Assumptions 3.2 and 3.3 hold. Moreover, given $\mathbf{Q}_{\ell,k}^{-\frac{1}{2}}$ in (6), define*

$$\hat{\mathbf{d}}_k := -\mathbf{P}_k \mathbf{Q}_{\ell,k}^{-\frac{1}{2}} \mathbf{R}_k \nabla f(\mathbf{x}_k),$$

and suppose that the sequence $(\mathbf{x}_k)_{k \in \mathbb{N}}$ is generated by $\mathbf{x}_{k+1} = \mathbf{x}_k + \frac{\xi^2 m}{L\sqrt{M}\omega^4} \hat{\mathbf{d}}_k$. Then, there exists $\hat{c} \in (0, 1)$ such that

$$f(\mathbf{x}_{k+1}) - f(\mathbf{x}^*) \leq \hat{c}(f(\mathbf{x}_k) - f(\mathbf{x}^*)).$$

Moreover, at most

$$\hat{K} = \frac{\log(f(\mathbf{x}_0) - f(\mathbf{x}^*)/\epsilon)}{\log(1/\hat{c})}$$

iterations are required for this process to reach accuracy ϵ .

Proof. Recall from the statement of the theorem that the sequence is generated by $\mathbf{x}_{k+1} = \mathbf{x}_k + t_k \hat{\mathbf{d}}_k$, where $\hat{\mathbf{d}}_k = -\mathbf{P}_k \mathbf{Q}_{\ell,k}^{-\frac{1}{2}} \mathbf{R}_k \nabla f(\mathbf{x}_k)$, $t_k = \frac{\xi^2 m}{\omega^4 L\sqrt{M}}$ and $\mathbf{Q}_{\ell}^{-1/2}$ is defined in (6). We also define the following quantity

$$\hat{\lambda}(\mathbf{x}) := \sqrt{\nabla f(\mathbf{x})^T \mathbf{P} \mathbf{Q}_{\ell}^{-\frac{1}{2}} \mathbf{R} \nabla f(\mathbf{x})}.$$

It holds $\hat{\lambda}(\mathbf{x}) \geq 0$. Below, we collect two general results that will be useful later in the proof. Given the Lipschitz continuity in Assumption 3.1 one can prove the following inequality (Nesterov et al. [2018]):

$$f(\mathbf{y}) \leq f(\mathbf{x}) + \nabla f(\mathbf{x})^T (\mathbf{y} - \mathbf{x}) + \frac{L}{2} \|\mathbf{y} - \mathbf{x}\|_2^2 \quad (7)$$

Similarly, from the strong convexity we can obtain

$$f(\mathbf{y}) \leq f(\mathbf{x}) + \nabla f(\mathbf{x})^T (\mathbf{y} - \mathbf{x}) + \frac{1}{2\mu} \|\nabla f(\mathbf{x}) - \nabla f(\mathbf{y})\|_2^2$$

Replacing \mathbf{y} and \mathbf{x} with \mathbf{x}_k and \mathbf{x}^* , respectively, we have that

$$f(\mathbf{x}_k) - f(\mathbf{x}^*) \leq \frac{1}{2\mu} \|\nabla f(\mathbf{x}_k)\|_2^2 \quad (8)$$

Furthermore, by construction, $\mathbf{Q}_{\ell,k}$ is bounded. It is bounded from below by m from (5) and it is bounded from above by the Lipschitz continuity of the gradients. Then, there exists $M \geq m > 0$ such that for all $k \geq 1$ we have that

$$m\mathbf{I} \preceq \mathbf{Q}_{\ell,k} \preceq M\mathbf{I}$$

The above inequality implies

$$\frac{1}{\sqrt{M}} \mathbf{P}_k \mathbf{R}_k \preceq \mathbf{P}_k \mathbf{Q}_{\ell,k}^{-\frac{1}{2}} \mathbf{R}_k \preceq \frac{1}{\sqrt{m}} \mathbf{P}_k \mathbf{R}_k$$

Using the above inequality we can obtain the following bound

$$\|\hat{\mathbf{d}}_k\|_2 = \|\mathbf{P}_k \mathbf{Q}_{\ell,k}^{-\frac{1}{2}} \mathbf{R}_k \nabla f(\mathbf{x}_k)\|_2 \leq \|\mathbf{P}_k \mathbf{Q}_{\ell,k}^{-\frac{1}{2}} \mathbf{R}_k\|_2 \|\nabla f(\mathbf{x}_k)\|_2 \leq \frac{1}{\sqrt{m}} \|\mathbf{P}_k \mathbf{R}_k\|_2 \|\nabla f(\mathbf{x}_k)\|_2 \leq \frac{\omega^2}{\sqrt{m}} \|\nabla f(\mathbf{x}_k)\|_2. \quad (9)$$

Similarly we can show a lower bound on $\hat{\lambda}(\mathbf{x})$

$$\hat{\lambda}(\mathbf{x})^2 = \nabla f(\mathbf{x})^T \mathbf{P} \mathbf{Q}_{\ell}^{-\frac{1}{2}} \mathbf{R} \nabla f(\mathbf{x}) \geq \frac{1}{\sqrt{M}} \|\mathbf{R} \nabla f(\mathbf{x})\|_2^2 \geq \frac{\xi^2}{\sqrt{M}} \|\nabla f(\mathbf{x}_k)\|_2^2, \quad (10)$$

Table 1: Mean training error and standard deviation for the Non-Linear Least-Squares problem. The results were obtained over 5 runs for random initialization from $\mathcal{N}(0, 1)$.

Algorithm	Mean \pm Std
Adam	0.0158 \pm 0.0016
AdaHessian	0.0325 \pm 0.0029
Simba	0.0097 \pm 0.001
Apollo	0.0556 \pm 0.0018

where the last inequality follows from Assumption 3.3. Using now (7) and the fact that $\hat{\lambda}(\mathbf{x})^2 = -\nabla f(\mathbf{x})^T \hat{\mathbf{d}}_k$ we take

$$f(\mathbf{x}_{k+1}) \leq f(\mathbf{x}_k) - t_k \hat{\lambda}(\mathbf{x}_k)^2 + t_k^2 \frac{L}{2} \|\hat{\mathbf{d}}_k\|_2^2.$$

Combining the above inequality with (10) and (9) we have that

$$\begin{aligned} f(\mathbf{x}_{k+1}) &\leq f(\mathbf{x}_k) - t_k \frac{\xi^2}{\sqrt{M}} \|\nabla f(\mathbf{x})\|_2^2 + t_k^2 \frac{L\omega^4}{2m} \|\nabla f(\mathbf{x}_k)\|_2^2 \\ &= f(\mathbf{x}_k) - \frac{\xi^4 m}{2\omega^4 M L} \|\nabla f(\mathbf{x}_k)\|_2^2, \end{aligned}$$

where the last inequality follows by the definition of t_k . Adding and subtracting $f(\mathbf{x}^*)$ on the above relationship and incorporating inequality (8) we obtain

$$f(\mathbf{x}_{k+1}) - f(\mathbf{x}^*) \leq \hat{c}(f(\mathbf{x}_k) - f(\mathbf{x}^*)),$$

where $\hat{c} := 1 - \frac{\xi^4 m \mu}{\omega^4 M L}$. Since $\xi < \omega, m < M$ and $\mu < L$ we take $\hat{c} \in (0, 1)$. Unravelling the last inequality we get

$$f(\mathbf{x}_k) - f(\mathbf{x}^*) \leq \hat{c}^k (f(\mathbf{x}_0) - f(\mathbf{x}^*)),$$

and thus $\lim_{k \rightarrow \infty} f(\mathbf{x}_k) = f(\mathbf{x}^*)$. Finally, solving for k the inequality $\hat{c}^k (f(\mathbf{x}_0) - f(\mathbf{x}^*)) \leq \epsilon$, we conclude that at least

$$\hat{K} = \frac{\log(f(\mathbf{x}_0) - f(\mathbf{x}^*)/\epsilon)}{\log(1/\hat{c})}$$

steps are required for this process to achieve accuracy ϵ . \square

A direct consequence of the above theorem is convergence in expectation when $(\mathbf{x}_k)_{k \geq 1}$ is generated randomly via a random prolongation matrix, e.g., see Definition 2.1. In this case we can guarantee that

$$\mathbb{E}[f(\mathbf{x}_k)] - f(\mathbf{x}^*) \leq \hat{c}^k (f(\mathbf{x}_0) - f(\mathbf{x}^*)),$$

which implies that $\lim_{k \rightarrow \infty} \mathbb{E}[f(\mathbf{x}_k)] = f(\mathbf{x}^*)$. Theorem 3.4 effectively shows the number of steps required for the method to reach the desired accuracy when the coarse direction is always effective. However, this may not be always true, which, in deterministic settings, implies no progress for the method. As discussed previously ξ and e can be viewed as user-defined parameters that prevent the method from taking the ineffective coarse steps. Given fixed ξ and e , the method performs iterations in the fine level if one of the two conditions in Assumption 3.3 is violated. In the fine level, the method constructs the preconditioner as follows

$$\mathbf{Q}_k := \nabla f(\mathbf{x}_k) \nabla f(\mathbf{x}_k)^T,$$

and then $\mathbf{Q}_k^{-\frac{1}{2}}$ is constructed exactly as in $\mathbf{Q}_{\ell,k}$ in (6). The next theorem shows a linear rate and derives the number of steps required when the method takes only fine steps.

Theorem 3.5. *Let $f : \mathbb{R}^n \rightarrow \mathbb{R}$ be a function such that Assumption 3.1 holds. Suppose also that Assumption 3.2 holds. Moreover, define*

$$\mathbf{d}_k := -\mathbf{Q}_k^{-\frac{1}{2}} \nabla f(\mathbf{x}_k),$$

and suppose that the sequence $(\mathbf{x}_k)_{k \in \mathbb{N}}$ is generated by $\mathbf{x}_{k+1} = \mathbf{x}_k + \frac{m}{L\sqrt{M}} \hat{\mathbf{d}}_k$. Then, there exists $c \in (0, 1)$ such that

$$f(\mathbf{x}_{k+1}) - f(\mathbf{x}^*) \leq c(f(\mathbf{x}_k) - f(\mathbf{x}^*)).$$

Moreover, at most

$$K = \frac{\log(f(\mathbf{x}_0) - f(\mathbf{x}^*)/\epsilon)}{\log(1/c)}$$

iterations are required for this process to reach accuracy ϵ .

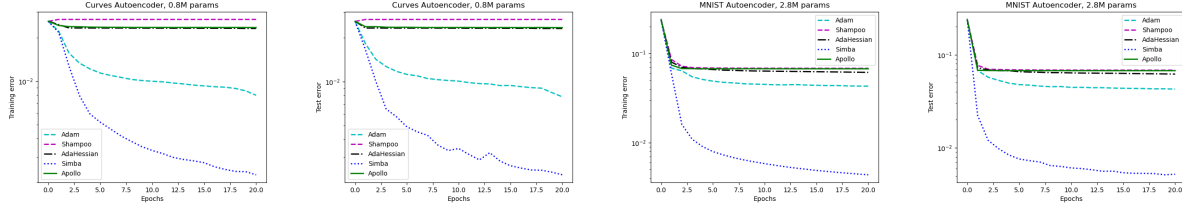


Figure 2: Convergence behaviour of various algorithms for the CURVES and MNIST autoencoders.

Table 2: Mean training error and standard deviation over 20 and 5 runs for the CURVES and MNIST autoencoders, respectively. The last column reports the wall-clock time for a single run of the two autoencoders problem.

Algorithm	CURVES	MNIST	Seconds CURVES/MNIST
Adam	0.0057 ± 0.0017	0.0431 ± 0.0007	22/176
AdaHessian	0.0165 ± 0.0049	0.0604 ± 0.0044	48/224
Shampoo	—	—	606/12,442
Apollo	0.02309 ± 0.00159	$0.0672 \pm 6.3 \times 10^{-7}$	31/197
Simba	0.00250 ± 0.0005	$0.0043 \pm 8.1 \times 10^{-5}$	54/467

Proof. The proof of theorem as it follows analogously to Theorem 3.4. The difference is the term that controls the linear rate which is now given by $c := 1 - \frac{m\mu}{ML}$. It holds $0 < \hat{c} \leq c < 1$. \square

As expected, theorem 3.5 shows a faster linear rate since the entire local information is employed during the training. Combining theorems 3.4 and 3.5, we provide the complete picture of the linear convergence rate of the proposed method.

4 Numerical Experiments

In this section we validate the efficiency of Simba to a number machine learning problems. Our goal is to illustrate that Simba outperforms the state-of-the-art diagonal optimization methods for problems with saddle points and flat areas or when the gradients are vanishing. For this purpose, we consider a non-linear least squares problems and two deep autoencoders where optimization methods often converge to suboptimal solutions. In addition, we demonstrate that our method is efficient and offers comparable, if not better, generalization errors compared to the state-of-the-art optimization methods on standard benchmark ResNets using CIFAR10 and CIFAR100 datasets.

Algorithms and set up: We compare Simba with momentum (algorithm 1) against Adam Kingma and Ba [2014], AdaHessian Yao et al. [2021], Apollo Ma [2020] and Shampoo Gupta et al. [2018] on a Tesla T4 GPU with a 16G RAM. The GPU time for Shampoo is not comparable to that of the other algorithm and hence its behaviour is reported only for the autoencoder problems. For all algorithms, the learning rate was selected using a grid search for $t_k \in \{1e-4, 5e-4, 1e-3, 5e-3, 1e-2, 5e-2, 1e-1, 5e-1, 1\}$. For all the algorithms we set the momentum parameters to their default values. For Simba we set $r = 20$ in all experiments. Through all the experiments the batch size is set to 128. For all algorithms we comprehensively tuned eps; the default value is selected when others do not yield an improvement. In our case we denote $m \equiv \text{eps}$.

4.1 Non-linear least-squares

Given a training dataset $\{\mathbf{a}_i, b_i\}_{i=1}^m$, $\mathbf{a}_i \in \mathbb{R}^n$ and $b_i \in \mathbb{R}$, we consider solving the following non-linear least-squares problem

$$\min_{\mathbf{x} \in \mathbb{R}^n} \frac{1}{m} \sum_{i=1}^m (b_i - g(\mathbf{a}_i^T \mathbf{x}))^2, \quad g(\omega) := \frac{1}{1 + \exp(\omega)},$$

which is a non-convex optimization problem. Here, we consider the Gisette dataset¹ for which $m = 6000$ and $n = 5000$. Furthermore, for Adam we select $t_k = 0.001$ and $\text{eps} = 10^{-8}$ while for Apollo we set $t_k = 0.01$ and $\text{eps} = 10^{-4}$. For AdaHessian, $t_k = 0.1$ and the hessian power parameter is set to 0.5. For Simba we select

¹Dataset available at: <https://www.csie.ntu.edu.tw/~cjlin/libsvmtools/datasets/binary.html>

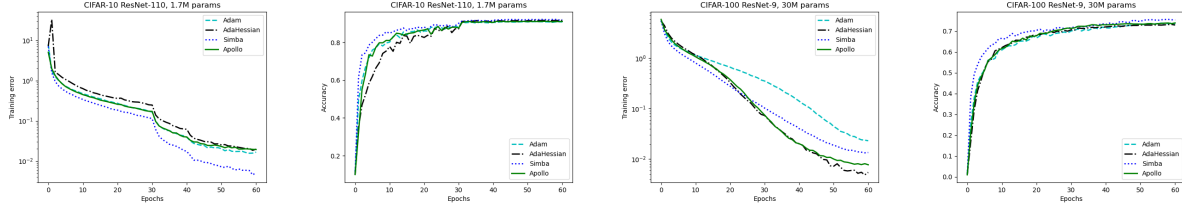


Figure 3: Convergence behaviour of various algorithms on CIFAR10 using ResNet110 and CIFAR100 using ResNet9.

Table 3: Mean training error and accuracy \pm standard deviation of various optimization algorithms over 5 on CIFAR10 and CIFAR100, respectively.

Algorithm	ResNet-110 - CIFAR10		ResNet-9 - CIFAR100	
	Training Error	Accuracy	Training Error	Accuracy
Adam	0.0284 ± 0.0060	91.03 ± 0.16	0.0237 ± 0.0005	73.91 ± 0.18
AdaHessian	0.0560 ± 0.0427	91.34 ± 1.04	0.0081 ± 0.0036	72.93 ± 0.66
Apollo	0.0315 ± 0.0066	91.18 ± 0.25	0.0076 ± 0.0003	73.70 ± 0.19
Simba	0.0097 ± 0.0023	92.07 ± 0.09	0.0133 ± 0.0001	75.41 ± 0.22

$n_\ell = 250$, $t_k = 0.05$ and $\text{eps} = 10^{-12}$. The performance of optimization methods appear in Figure 1. Observe that this problems has several flat areas or saddle points which slow down the convergence of all algorithms. Nevertheless, the method with the best behaviour is Simba which enjoys a much faster escape rate from the saddle points and thus always returns lower training errors. This can be also observed for different initialization points. In Table 1 we report the average training error and the standard deviation over 5 runs. The method that comes closer to Simba is Adam. Further, from Figure 1 we see that, although the wall-clock time of Simba is two to three times increased compared to its competitors, the total time of our method is much better due to its fast escape rate near saddles and flat areas. Further, in Figure 4 in the supplementary material we compare the performance of Simba for different sizes in the coarse model. We observed that even Simba with $n_\ell = 25$ (i.e., updating only 25 parameters at each iteration) enjoys better escape rate than its competitors. This indicates that diagonal methods perform poorly near saddles and flat areas and highlights the importance of constructing meaningful preconditioners. Moreover, observe that the best wall-clock time is achieved with only 5% of the dimensions. This indicates that Simba significantly reduces the computational cost of preconditioned methods without compromising the convergence rate.

4.2 Deep autoencoders

In this section we investigate the performance of Simba on two deep autoencoder optimization problems that arise from (Hinton and Salakhutdinov [2006]), named CURVES and MNIST. Both optimization problems are considered difficult to solve and have become a standard benchmark for optimization methods due to the presence of saddle points and the issue of the vanishing gradients. The CURVES² autoencoder consists of an encoder with layer size $28 \times 28, 400, 200, 100, 50, 25, 6$, a symmetric decoder which totals to 0.8M parameters. For all layers the relu activation function is applied. The network was trained on 20,000 images and tested on 10,000. We set the learning rate equal to 0.001, 1, 0.05, 0.5 and 0.01 for Adam, Apollo, AdaHessian, Shampoo and Simba, respectively. The eps parameter is selected 10^{-15} and 10^{-8} for Apollo and Simba, respectively, and set to its default value for the rest algorithms. The hessian power parameter for AdaHessian is selected 1. Further, the MNIST³ autoencoder consists of an encoder with layer size $28 \times 28, 1000, 500, 250, 30$ and a symmetric decoder which totals to 2.8M parameters. In this network we use the sigmoid activation function to all layers. The training set for the MNIST dataset consists of 60,000 images while the test set has 10,000 images. Here, t_k is set equal to 0.001, 0.9, 0.1, 0.05 and 0.05 for Adam, Apollo, AdaHessian, Shampoo and Simba, respectively. The eps parameter is set equal to 10^{-8} for Simba and to its default value for all other algorithms; the hessian power of AdaHessian is set equal to 1. For both autoencoder problems the coarse model size parameter is set $n_\ell = 0.5N$.

The comparison between the optimization algorithms for the two deep autoencoders appears in Table 2 and Figure 2. Clearly, Simba performs the best among the optimization algorithms resulting in the lowest training error in both CURVES and MNIST autoencoders. As a result, Simba performs better than its competitors on the test set too. It is evident that all the other methods get stuck in stationary points with large errors. In these points we observed that the

²Dataset available at: www.cs.toronto.edu/~jmartens/digs3pts_1.mat

³Dataset available at: <https://pytorch.org/vision/main/datasets.html>

gradients become almost zero which results in a very slow progress of Adam, AdaHessian, Apollo and Shampoo. On the other, Simba enjoys a very fast escape rate from such points and thus it yields a very fast decrease in the training error. In addition, Table 2 reports the wall-clock time for each optimization algorithm. We see that Simba has an increased per-iteration costs (by a factor between two and three compared to Adam), nevertheless this is a reasonable price to pay for achieving a good decrease in the value function. The averaged behaviour of Shampoo is missing due to its expensive iterations. For this reason we omit Shampoo from the following experiments.

4.3 Residual Neural Networks

In this section we report comparisons on the convergence and generalization performance between the optimization algorithms using ResNet110⁴ and ResNet9⁵ with CIFAR-10 and CIFAR-100 datasets, respectively. ResNet110 consists of 110 layers and a total of 1.7M parameters while ResNet9 has 9 layers and 30M parameters. Hence, our goal is to investigate the performance of Simba on benchmark problems and different architectures, i.e., deep and wide networks.

For ResNet110 we set an initial learning rate parameter equal to 0.001, 0.1, 0.1, 0.01 for Adam, Apollo, AdaHessian and Simba, respectively. We train the network for a total number of 60 epochs and decrease the learning rate by a factor of 5 at epochs 30 and 40. The hessian power parameter for AdaHessian is selected 1 and for Simba the hyper-parameter eps is set to 10^{-8} while $n_\ell = 0.5N$. The convergence and generalization performance between the optimization algorithms is illustrated in Figure 3 and Table 3. We see that Simba is able to achieve results that are comparable, if not better, with that of Adam, AdaHessian and Apollo in both training and generalization errors. The total GPU time of Simba is about three times larger than that of Adam, which is the fastest algorithm, but it is considerably smaller than that of AdaHessian (see Figure 5 in the supplement).

For ResNet9, we set an initial value on t_k as follows: 0.0005, 0.001, 0.05, 0.005 for Adam, Apollo, AdaHessian and Simba, respectively. We train the network for 60 epochs and use cosine annealing to determine the learning rate at each epoch and set minimum t_k value equal to $0.01t_k$, $0.1t_k$, $0.01t_k$, $0.02t_k$ for Adam, Apollo, AdaHessian and Simba, respectively. The hessian power, eps and n_ℓ parameters are set as above. Since classifying CIFAR100 is a much more difficult problem than CIFAR10, to improve the accuracy we use weight decay and gradient clipping with values fixed at 0.001 and 0.01, respectively, for all algorithms. Figure 3 and Table 3 indicate that Simba is able to offer very good generalization results on a difficult task. Further, we see that Simba is less than two times slower in wall-clock time than Adam and Apollo but again considerably faster than AdaHessian (see Figure 6 in the supplement). Figure 6 also shows that the total GPU time of Simba for reaching the desired classification accuracy is comparable to that of Adam and Apollo which indicates the efficiency of our method on large-scale optimization problems.

5 Conclusions

We present Simba, a scalable bilevel optimization algorithm to address the limitations of first-order methods in non-convex settings. We demonstrate the fast escape rate from saddles of our method through empirical evidence. Numerical results also indicate that Simba achieves good generalization errors on modern machine learning applications. Convergence guarantees of Simba when locally assume convex functions are also established. As a future work, we aim to apply Simba for the training of LLMs such as GPT.

References

- Yann N Dauphin, Razvan Pascanu, Caglar Gulcehre, Kyunghyun Cho, Surya Ganguli, and Yoshua Bengio. Identifying and attacking the saddle point problem in high-dimensional non-convex optimization. *Advances in neural information processing systems*, 27, 2014.
- Ioannis Panageas, Georgios Piliouras, and Xiao Wang. First-order methods almost always avoid saddle points: The case of vanishing step-sizes. *Advances in Neural Information Processing Systems*, 32, 2019.
- Yurii Nesterov et al. *Lectures on convex optimization*, volume 137. Springer, 2018.
- Stephen Boyd and Lieven Vandenberghe. *Convex optimization*. Cambridge University Press, Cambridge, 2004. ISBN 0-521-83378-7. doi:10.1017/CBO9780511804441. URL <https://doi.org/10.1017/CBO9780511804441>.
- Yurii Nesterov. *Introductory lectures on convex optimization*, volume 87 of *Applied Optimization*. Kluwer Academic Publishers, Boston, MA, 2004. ISBN 1-4020-7553-7. doi:10.1007/978-1-4419-8853-9. URL <https://doi.org/10.1007/978-1-4419-8853-9>. A basic course.

⁴Network implementation available at: https://github.com/akamaster/pytorch_resnet_cifar10

⁵Network implementation available at: <https://www.kaggle.com/code/yiweiwangau/cifar-100-resnet-pytorch-75-17-accuracy>

- John Duchi, Elad Hazan, and Yoram Singer. Adaptive subgradient methods for online learning and stochastic optimization. *Journal of machine learning research*, 12(7), 2011.
- Tijmen Tieleman, Geoffrey Hinton, et al. Lecture 6.5-rmsprop: Divide the gradient by a running average of its recent magnitude. *COURSERA: Neural networks for machine learning*, 4(2):26–31, 2012.
- Matthew D Zeiler. Adadelta: an adaptive learning rate method. *arXiv preprint arXiv:1212.5701*, 2012.
- Diederik P Kingma and Jimmy Ba. Adam: A method for stochastic optimization. *arXiv preprint arXiv:1412.6980*, 2014.
- Manzil Zaheer, Sashank Reddi, Devendra Sachan, Satyen Kale, and Sanjiv Kumar. Adaptive methods for nonconvex optimization. *Advances in neural information processing systems*, 31, 2018.
- Zhewei Yao, Amir Gholami, Sheng Shen, Mustafa Mustafa, Kurt Keutzer, and Michael Mahoney. Adahessian: An adaptive second order optimizer for machine learning. In *proceedings of the AAAI conference on artificial intelligence*, volume 35, pages 10665–10673, 2021.
- Xuezhe Ma. Apollo: An adaptive parameter-wise diagonal quasi-newton method for nonconvex stochastic optimization. *arXiv preprint arXiv:2009.13586*, 2020.
- Majid Jahani, Sergey Rusakov, Zheng Shi, Peter Richtárik, Michael W Mahoney, and Martin Takáč. Doubly adaptive scaled algorithm for machine learning using second-order information. *arXiv preprint arXiv:2109.05198*, 2021.
- Hong Liu, Zhiyuan Li, David Hall, Percy Liang, and Tengyu Ma. Sophia: A scalable stochastic second-order optimizer for language model pre-training. *arXiv preprint arXiv:2305.14342*, 2023.
- Charles G Broyden. Quasi-newton methods and their application to function minimisation. *Mathematics of Computation*, 21(99):368–381, 1967.
- Murat A Erdogdu and Andrea Montanari. Convergence rates of sub-sampled newton methods. In *Proceedings of the 28th International Conference on Neural Information Processing Systems-Volume 2*, pages 3052–3060. MIT Press, 2015.
- Mert Pilanci and Martin J Wainwright. Newton sketch: A near linear-time optimization algorithm with linear-quadratic convergence. *SIAM Journal on Optimization*, 27(1):205–245, 2017.
- Peng Xu, Jiyan Yang, Farbod Roosta-Khorasani, Christopher Ré, and Michael W Mahoney. Sub-sampled newton methods with non-uniform sampling. In *Advances in Neural Information Processing Systems*, pages 3000–3008, 2016.
- Peng Xu, Fred Roosta, and Michael W Mahoney. Second-order optimization for non-convex machine learning: An empirical study. In *Proceedings of the 2020 SIAM International Conference on Data Mining*, pages 199–207. SIAM, 2020.
- Vineet Gupta, Tomer Koren, and Yoram Singer. Shampoo: Preconditioned stochastic tensor optimization. In *International Conference on Machine Learning*, pages 1842–1850. PMLR, 2018.
- Nick Tsipinakis and Panos Parpas. A multilevel method for self-concordant minimization. *arXiv preprint arXiv:2106.13690*, 2021.
- Nick Tsipinakis, Panagiotis Tigkas, and Panos Parpas. A multilevel low-rank newton method with super-linear convergence rate and its application to non-convex problems. *arXiv preprint arXiv:2305.08742*, 2023.
- N. Halko, P. G. Martinsson, and J. A. Tropp. Finding structure with randomness: probabilistic algorithms for constructing approximate matrix decompositions. *SIAM Rev.*, 53(2):217–288, 2011. ISSN 0036-1445. doi:10.1137/090771806. URL <https://doi.org/10.1137/090771806>.
- Sébastien Bubeck et al. Convex optimization: Algorithms and complexity. *Foundations and Trends® in Machine Learning*, 8(3-4):231–357, 2015.
- Sashank Reddi, Manzil Zaheer, Suvrit Sra, Barnabas Poczos, Francis Bach, Ruslan Salakhutdinov, and Alex Smola. A generic approach for escaping saddle points. In *International conference on artificial intelligence and statistics*, pages 1233–1242. PMLR, 2018.
- Thomas O’Leary-Roseberry, Nick Alger, and Omar Ghattas. Low rank saddle free newton: A scalable method for stochastic nonconvex optimization. *arXiv preprint arXiv:2002.02881*, 2020.
- James Martens and Roger Grosse. Optimizing neural networks with kronecker-factored approximate curvature. In *International conference on machine learning*, pages 2408–2417. PMLR, 2015.
- Chin Pang Ho, Michal Kočvara, and Panos Parpas. Newton-type multilevel optimization method. *Optimization Methods and Software*, pages 1–34, 2019.

- Yurii Nesterov and Boris T Polyak. Cubic regularization of newton method and its global performance. *Mathematical Programming*, 108(1):177–205, 2006.
- Santiago Paternain, Aryan Mokhtari, and Alejandro Ribeiro. A newton-based method for nonconvex optimization with fast evasion of saddle points. *SIAM Journal on Optimization*, 29(1):343–368, 2019.
- Geoffrey E Hinton and Ruslan R Salakhutdinov. Reducing the dimensionality of data with neural networks. *science*, 313(5786):504–507, 2006.

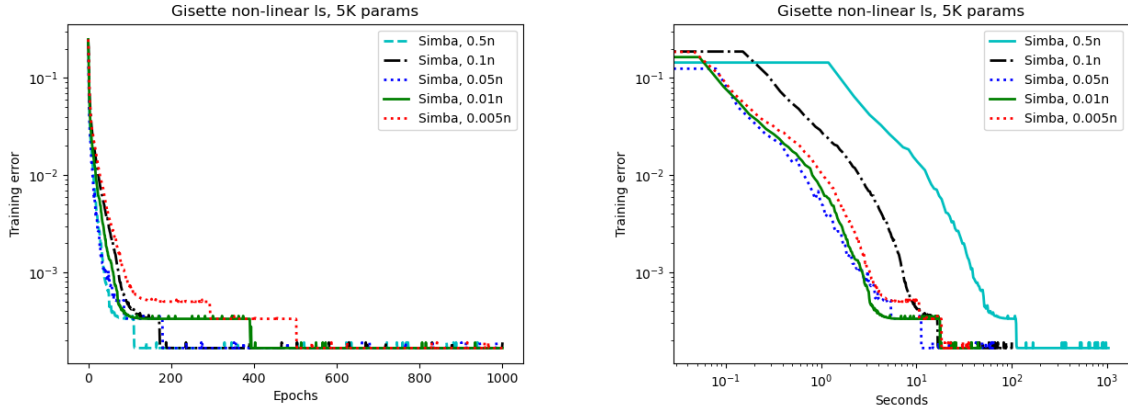


Figure 4: Convergence behaviour of Simba for different coarse models. In all cases Simba is initialized at the origin. The parameter r is set to 10 for $n_\ell = 0.005N$ and 20 otherwise. Further, t_k is selected 0.01 for $n = 0.5N$ or $n = 0.1N$ and 0.05 otherwise. Interestingly, we see that Simba with $n = 25$ matches the performance of Simba that use much larger coarse models. Note that, by Definition 2.1, Simba only updates 25 parameters at each iteration which indicates that near saddles and flat areas one should employ more informative directions than those of the first-order methods with second-order momentum. As expected, we see that a better convergence and escape rate is expected for larger coarse models but this comes at the cost of more expensive iterations. The figure shows that Simba with $n = 250$ has the best total complexity.

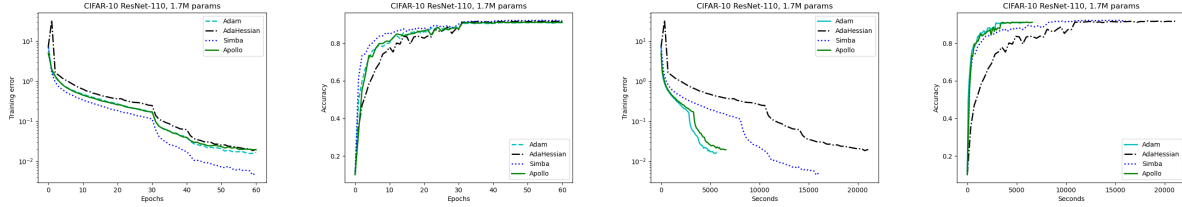


Figure 5: Convergence behaviour and wall-clock time of various algorithms on CIFAR10 using ResNet110.

A Extra Numerical Results

Here, we report some extra numerical results. Figure 4 shows how the size of the coarse model affects the convergence behaviour of Simba on the non-linear least squares problem. Additionally, Figures 5 and 6 show the wall-clock time for training the residual neural networks for 60 epochs.

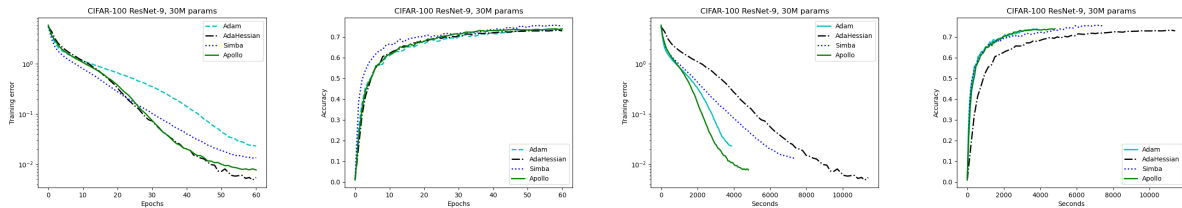


Figure 6: Convergence behaviour and wall-clock time of various algorithms on CIFAR100 using ResNet9.